SEMARAK ILMU PUBLISHING

Journal of Advanced Research in Numerical Heat Transfer

Journal homepage:
https://semarakilmu.com.my/journals/index.php/arnht/index
ISSN: 2735-0142

Optimizing Heat Transfer: Corrugated Backward First Step Integration with Obstacles for Enhanced Performance

Taghreed Kadom Sarhan[1,*], Mohd Khairol Anuar Mohd Ariffin[1,♣], Eris Elianddy Supeni[1], Kamarul Arifin Ahmad[2], Abd. Rahim Abu Talib[2], Razi Al-Zubaidi[3]

[1] Department of Mechanical Engineering, Faculty of Engineering, Universiti Putra Malaysia (UPM), 43400, Serdang, Selangor, Malaysia
[2] Department of Aerospace Engineering, Faculty of Engineering, Universiti Putra Malaysia (UPM), 43400, Serdang, Selangor, Malaysia
[3] Lincoln University College, 47301, Petaling Jaya, Selangor, Malaysia

ARTICLE INFO

Article history:
Received 22 December 2024
Received in revised form 25 January 2025
Accepted 24 February 2025
Available online 30 March 2025

Keywords:
Backward-Facing Step (BFS); heat transfer; flow separation; turbulence; recirculation zones

ABSTRACT

In this study, we investigate how heat transfer enhancement can be achieved in backward facing step (BFS) channels with corrugated bottoms and strategically placed obstacles via using water as base fluid. Simulations were performed using the Finite Volume Method (FVM) and SIMPLE method. The upstream dimension is 200 mm, the downstream dimension is 300 mm, and height varies from 10 mm at the inlet to 20 mm at the outlet. Four obstacle configurations were analyzed: Model A of 2.5 mm obstacle; Model B of 5 mm obstacle; Model C of 5 mm obstacle at 30°; Model D of three 5 mm obstacles. Reynolds numbers (Re) from 5000 to 20,000 and a constant heat flux of 40 kW/m² were studied. Model B with a trapezoidal corrugated bottom and 5 mm obstacle 215 mm from the inlet had the Nusselt number (Nu) and optimized performance evaluation criteria (PEC) demonstrated up to a 90% improvement over smooth BFS and 20% over trapezoidal BFS in heat transfer. Increasing turbulence and recirculation also helped improve fluid mixing and wall heat transfer through effective obstacle positioning. For BFS channels, Model B offered the best trade off of heat transfer enhancement and frictional losses, and thus represented the best design for thermal performance optimization.

1. Introduction

Backward-facing step (BFS) is an important geometric feature in fluid dynamics and heat transfer research used to optimize heat exchanger performance in various industrial applications, such as combustion devices to electronic cooling [1-3]. Fundamental to its ability to induce flow separation and reattachment is that it profoundly affects fluid flow phenomena, such as turbulence and mixing, and so, it must be used to enhance its heat transfer characteristics [4-8].

* *Corresponding author.*
E-mail address: tagreedkadom22@gmail.com (Taghreed Kadom Sarhan)
♣ *Corresponding author.*
E-mail address: khairol@upm.edu.my (Mohd Khairol Anuar Mohd)

https://doi.org/10.37934/arnht.31.1.5675

Downstream of a BFS, a recirculation zone develops that increases mixing and turbulence to enhance fluid mixing in the flow and thereby improve heat transfer rates. In particular, this effect is evident in studies considering non-Newtonian nanofluid flows under non Boussinesq conditions [9-11]. where BFS strongly affects flow and heat transfer structures. Additionally, the BFS configuration affects shock and vortex characteristics in high-speed environments as in supersonic flows, which improves jet mixing and extends penetration depth and mixing efficiency needed for scramjet developments [12].

Height and shape geometric parameters of the BFS affect the flow dynamics and heat transfer efficiency. For instance, there are more pronounced recirculation zones (zones of reduced flow) which enhance mixing for supersonic flows with larger step heights [10,12,13]. Moreover, the critical Reynolds number and bottom wall length play a crucial role in flow instability. Thus, the parameters that drive such a transition of flow between steady and unsteady can also further increase heat transfer by increased turbulence [7,14,15].

Specifically, in cooling systems for turbines and scramjets, where high effective heat transfer is required for overall performance and efficiency, BFS configurations are critical [16]. These configurations can be used strategically to maximize heat transfer through complex geometries, such as dual step cylinders and channels with rough surface surfaces [8,17,18].

But unlike the BFS, the improved heat transfer comes with increased complexity in flow dynamics, such as increased drag and pressure losses which must be carefully managed in practical use [10,17]. Moreover, interactions between the synthesized vortex array of BFS and other flow features, such as forward facing steps, can generate intricate flow patterns which require the application of advanced modelling techniques to ensure good predictability [7,19].

This extends the understanding far beyond isothermal conditions to a spectrum of parameters governing the fluid and channel geometry.

1.1 Impact of Corrugated Walls on Heat Transfer Enhancement

Corrugated walls integrated into heat exchanger design have shown consistently to enhance heat transfer efficiency, at least occasionally at the expense of increased pressure drop. Heat transfer and fluid dynamics in backward facing step (BFS) channels are shown to be dependent on step height in the studies. As shown by Azeez *et al.,* [20] and Ekiciler *et al.,* [4], other researchers [3,21,22] reported that heat transfer performance can be improved when corrugated walls are used in BFS channels.

Experimentally Abedalh *et al.,* [23] studied hybrid nanofluids (Al2O3 and TiO2 nanoparticles in water) and demonstrated an 14% increase in heat transfer over BFS duct, and an remarkable 16% increase in Nusselt number with a 3% mass fraction. As with Ekiciler *et al.,* [4], SiO2-water nanofluid flow over a corrugated BFS step was explored, and it was found that an optimal heat transfer performance is achieved at a nanoparticle volume fraction of 3.0% at a Reynolds number of 240. Improvements in fluid flow and heat transfer on all surfaces were apparent in Koca [21] numerical exploration of a corrugated channel with a backward-facing step. Best Performance Evaluation Criteria (PEC) values for the 20 mm triangular bottom surface (as compared to the 10 mm triangular bottom surface) were found at Re = 5 × 10^3 and Re = 10^4.

The works of Selimefendigil *et al.,* [22] confirmed the effectiveness of corrugated walls as they reported increase of 5.20% in the average Nusselt number from Reynolds numbers of 10 to 200. Azeez *et al.,* [20] also demonstrated using numerical simulations that heat transfer efficiency can be increased significantly, by a factor of 30%, using aluminium nitride nanofluid at a 4% nanoparticle fraction in trapezoidal channels.

The heat transfer characterization of MWCNT-Fe3O4/water hybrid nanofluid in a channel with a backward facing step and with a top wall baffle was examined by Ma *et al.,* [24]. Nusselt numbers decreased as baffles were lengthened and nanoparticle fractions had little effect on flow. Heat transfer rates were greatly affected by changing baffle position and length. According to Saleem *et al.,* [25], increasing Reynolds numbers in an open channel with BFS were associated with increased vortex shedding and complex interactions between flow velocity or turbulence.

Selimefendigil *et al.,* [26] conducted research that showed an increase in local heat transfer of 6.66 percent over obstacle configurations of no obstacles. This is also the case in corrugated walls for heat pipes, in which their wavy structure permits the engagement of capillary action and thermal expansion accommodation to enhance at least on thermal management [27].

Overall, corrugated walls increase surface area and improve fluid dynamics, while improving heat transfer overall. As seen in double pipe heat exchangers, corrugations can increase the convective heat transfer coefficient; Nusselt numbers reaching 2.17 times the value in smooth tube [28]. Corrugated walls in two phase flow systems facilitate recirculing flows to accelerate transitions and reduce bubble sizes, which further confirm improved heat [29].

Other geometric modifications such as "Λ"- and "V"-shaped inclinations are also found to increase heat transfer by up to 32% by increasing surface area and modifying flow structure [30]. Further, circumferentially corrugated walls in double layered tubes break thermal boundary layers and thus, improve efficiency [31].

Research at last finally finds that the average Nusselt number in corrugated channels scales with Reynolds and Prandtl numbers, whereas heat transfer rates can be in excess of 120% of those in straight channels [32]. These results highlight the benefit of corrugated designs, in particular, V configurations to achieve the best energy savings and structural integrity in a wide range of engineering applications [33].

1.2 Effectiveness of Geometrical Modifications

It appears that Zheng *et al.,* [34], Mushatet [35], Xiao *et al.,* [36], Çelik *et al.,* [37], Hammoodi *et al.,* [38], Eleiwi *et al.,* [3], Alawi *et al.,* [15], and Menni *et al.,* [39] all studied different geometrical modifications, e.g., ribs, baffles, winglets, or barriers, undertaken in BFS channels to enhance turbulent heat transfer.

Heat transfer enhancement in ribbed channels of square cross-section was studied by Zheng *et al.,* [34]. Trough rectangular ribs a 160° inclined lee side structure had Nusselt numbers and friction factors increase approximately 4.6–6.4 % and 7.1–9.0 % respectively, with concomitant increase in heat transfer of 7.1–9.0 %. Although its heat transfer was superior, the inclined back wall geometry suffered from higher friction, and that hampered overall thermal performance. Similar work by Mushatet [35] explored turbulent flow and heat transfer over backward facing steps with rib turbulators. We found that an increase of the contraction ratio, characterized by a larger step height, favored recirculation zones behind the step, and consequently, a larger reduction of turbulent kinetic energy and Nusselt number variations. In addition, the heat transfer in heat exchangers has been improved through a variety of turbulator types. Hammoodi *et al.,* [38], and Menni *et al.,* [39] likely investigated various geometrical modifications—such as ribs, baffles, winglets, or barriers—in BFS channels to heighten turbulent heat transfer.

Zheng *et al.,* [34] explored heat transfer enhancement in ribbed channels with square cross-sections. They found that a 160° inclined lee-side structure outperformed rectangular ribs, resulting in Nusselt numbers and friction factors approximately 4.6%–6.4% higher, with a corresponding 7.1%–9.0% increase in heat transfer. However, despite superior heat transfer, the inclined back-wall

geometry exhibited higher friction, affecting overall thermal performance. Similarly, Mushatet [35] investigated turbulent flow and heat transfer over backward-facing steps with rib turbulators. Increasing the contraction ratio, marked by a higher step height, was found to enhance recirculation zones behind the step, with significant impacts on turbulent kinetic energy and Nusselt number variations. Furthermore, focused on improving heat transfer in heat exchangers through various turbulator types. The research revealed the significance of a range of design parameters, including attack angle and height, as important factors in improving heat transfer performance. Pressure loss and heat transfer efficiency can be reduced by incorporating variation in winglet angle with perforation forms. Hammoodi *et al.,* [38] also assessed the ability of oblique triangular ribs to control flow heat transfer in circular channels, showing substantial increases in cooling air temperature of 6.25%, 12.5%, and 17.5% in the first, second and third cases, respectively, and to enhance heat flow rate at Re =14000. Xiao *et al.,* [36] address the issue of enhancing turbulent heat transfer in mini channels by means of v-ribs, which create wall leading edge pressure gradients and facilitate mixing. Experimental results show that this design drastically improves the thermal performance over that of conventional smooth mini-channels. These findings indicate that maximizing heat transfer efficiency can be achieved by optimizing rib geometry and placement, v-ribs generate multi-longitudinal swirl flows, and improve the heat transfer coefficient and overall efficiency in compact heat exchangers. Addition, Menni *et al.,* [39] studied the optimal configuration for heat transfer. At higher Reynolds numbers, a more effective channel, with a flat fin and a 45^{o} V shaped baffle, is shown to have enhanced heat transfer and friction loss compared to smaller ones. High ratios of *Nu*/*Nu*0 and f/f0 are obtained under short separation distances between obstacles, while better performing cases are obtained with increased separation distances, they yield a larger thermal enhancement factor (TEF).

They may have evaluated the effect of these modifications on flow characteristics, heat transfer coefficients, and overall performance through experimental or numerical means. These modifications demonstrate the feasibility of inducing turbulence and enhancing heat transfer rates in heat exchangers and similar devices, providing valuable insights for the design optimization of such systems. Importantly, this study gains significance in its exploration of different approaches to improve heat transfer efficiency in backward-facing step (BFS) channels and, thereby, enhance heat exchanger performance—an issue critical to numerous industrial applications.

Although several advancements have been made, there remains a lack of comprehensive understanding of the heat transfer enhancement achieved through the combined use of corrugated channels and obstacles in BFS configurations. While individual geometric modifications, such as corrugated walls or obstacles, have been extensively studied, the interaction between these elements and their combined influence on flow dynamics and thermal performance has not been adequately explored. Moreover, the trade-offs between enhanced heat transfer efficiency and associated pressure losses, critical for practical applications, remain underreported. This gap restricts the ability to fully optimize BFS-based heat exchangers for industrial use.

This study aims to bridge this gap by investigating the combined impact of corrugated channels and obstacles on heat transfer performance in BFS configurations. Additionally, other promising avenues, such as dimpled surfaces and spiral generators, are explored for their potential to enhance heat transfer. Through experimental and numerical analyses, the study seeks to elucidate the complex fluid dynamics and heat transfer interactions within these modified geometries. The findings will provide actionable insights for optimizing heat exchanger designs, improving heat transfer efficiency, and guiding future research directions in thermal engineering.

2. Numerical Methodology

2.1 Physical Model and Assumptions

The flow configuration and geometry utilised in this study are depicted in Figure 1. To facilitate comprehensive flow growth inside the channel, the upstream wall length is established at L1=200 mm, while the downstream wall length is modified to L2+L3=300 mm. The inlet and outlet heights are h=10mm and H=20mm, respectively, yielding an expansion ratio of 2. In order to induce modifications in fluid flow, a small wing is introduced into the backward-facing step, resulting in a corrugated channel with obstacles, as depicted in Figure 1. The figure illustrates four various models (A), (B), (C), and (D) representing the backward-facing step of the corrugated channel with obstacles. These obstacles are positioned at different locations along the wall or within the middle of the channel and at varying angles.

i) Model (A): a backward-facing step (BFS) with corrugated bottom and an upper obstacle with a length of LW=2.5mm, an angle of 90 degree, and positioned 200mm from the fluid inlet (Figure 1(a)).
ii) Model (B): a backward-facing step (BFS) with corrugated bottom and an upper obstacle with a length of LW=5mm, an angle of 90 degree, and located 215mm from the inlet (Figure 1(b)).
iii) Model (C): a backward-facing step (BFS) with corrugated bottom and an upper obstacle with a length of LW=5mm, located 200mm from the inlet, and an angle of 30 degree (Figure 1(c)).
iv) Model (D): a backward-facing step (BFS) with corrugated bottom with three obstacles, each with a length of LW=5mm, angle of 90 degree, and positioned at distances of 200mm, 215mm, and 230mm from the fluid inlet, respectively (Figure 1(d)).

The step height (S=10mm), pitch diameter (P=20mm), and corrugated amplitude height (a=4mm) of the channel are referred to as P and a, respectively. A constant heat flux of 40 kW/m² is delivered to the lower wall across a length of L2=200 mm, while the remaining walls are treated as adiabatic surfaces. The investigation used pure water as the working fluid.

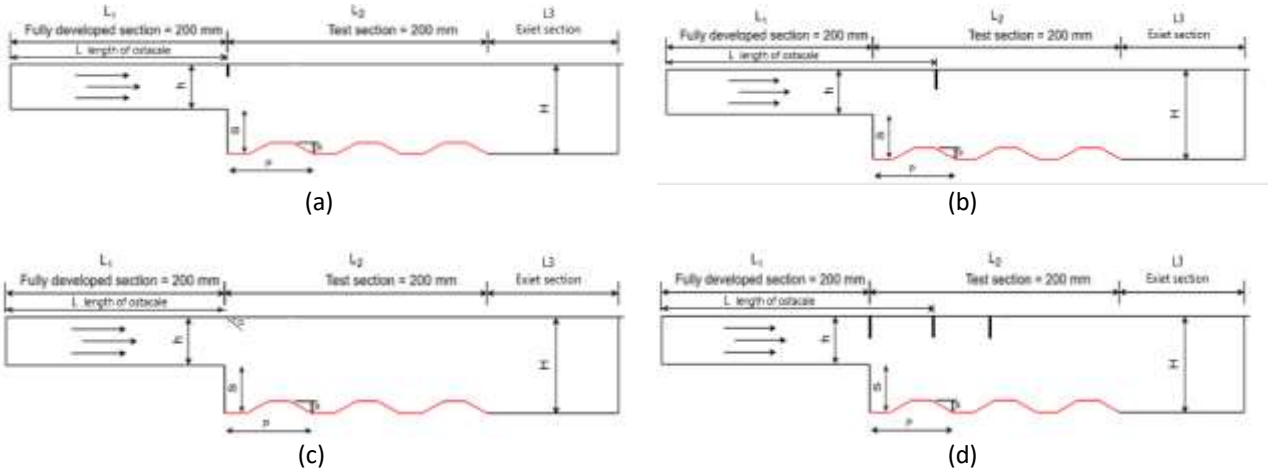

Fig. 1. (a) Model A, backward-facing step (BFS) with corrugated bottom and an upper obstacle with a length of LW=2.5mm, an angle of 90 degree, and positioned 200mm from the fluid inlet (b) Model B, backward-facing step (BFS) with corrugated bottom and an upper obstacle with a length of LW=5mm, an angle of 90 degree, and located 215mm from the inlet (c) Model C, backward-facing step (BFS) with corrugated bottom and an upper obstacle with a length of LW=5mm, located 200mm from the inlet, and an angle of 30 degree (d) Model D, backward-facing step (BFS) with corrugated bottom with three obstacles, each with a length of LW=5mm, angle of 90 degree, and positioned at distances of 200mm, 215mm, and 230mm from the fluid inlet, respectively

2.2 Governing Equations

The governing equations for continuity, momentum, and energy are solved to model turbulent flow under steady-state conditions in a two-dimensional, incompressible Newtonian fluid system with continuous flow. These equations are expressed as described in Eq. (1) – Eq. (5) as detailed by Hilo *et al.,* [40] and Taib *et al.,* [41].

The continuity equation:

$$\frac{\partial(\rho\bar{u})}{\partial x}+\frac{\partial(\rho\bar{v})}{\partial y}=0 \tag{1}$$

The x-Momentum equation:

$$\frac{\partial}{\partial x}(\rho\bar{u}\bar{u})+\frac{\partial}{\partial y}(\rho\bar{u}\bar{v})=-\frac{\partial P}{\partial x}+\frac{\partial}{\partial x}+\left[(\mu+\mu_t)\frac{\partial\bar{u}}{\partial x}\right]+\frac{\partial}{\partial y}\left[(\mu+\mu_t)\frac{\partial\bar{u}}{\partial y}\right] \tag{2}$$

The y-Momentum equation:

$$\frac{\partial}{\partial x}(\rho\bar{u}\bar{v})+\frac{\partial}{\partial y}(\rho\bar{v}\bar{v})=-\frac{\partial P}{\partial x}+\frac{\partial}{\partial x}+\left[(\mu+\mu_t)\frac{\partial\bar{v}}{\partial x}\right]+\frac{\partial}{\partial y}\left[(\mu+\mu_t)\frac{\partial\bar{v}}{\partial y}-\frac{2}{3}\rho\frac{\partial k}{\partial y}\right] \tag{3}$$

The conservation of energy equation:

$$\frac{\partial}{\partial x}(\rho\bar{u}T)+\frac{\partial}{\partial y}(\rho\bar{v}T)=\frac{\partial}{\partial x}\left[\left(\frac{k}{C_p}+\frac{\mu_t}{Pr_t}\right)\frac{\partial T}{\partial x}\right]+\frac{\partial}{\partial y}\left[\left(\frac{k}{C_P}+\frac{\mu_t}{Pr_t}\right)\frac{\partial T}{\partial y}\right] \tag{4}$$

The given equations feature symbols where ρ represents density, μ denotes kinematic viscosity, T signifies temperature, Cp stands for specific heat, and $\bar{u}$ and $\bar{v}$ represent dimensionless x and y

velocity components, respectively. The symbol μt denotes turbulent dynamic viscosity, also known as eddy viscosity, which correlates with k and ε, and its calculation is determined as follows:

$$\mu_t = \rho C_\mu f_\mu \left(\frac{k^2}{\varepsilon}\right) \tag{5}$$

To solve the governing equations and handle corresponding boundary conditions, the Finite Volume Method (FVM) was applied using the ANSYS-Fluent V.24 commercial Computational Fluid Dynamics (CFD) package. The use of ANSYS and SolidWorks aligns with Asral *et al.,* [42], demonstrating their effectiveness in thermal analyses.

The SIMPLE algorithm resolved the flow field, employing a second-order upwind differencing scheme for convection. The k-ε turbulent model with RNG was chosen to examine the turbulence flow over the channel, and the diffusion term in momentum and energy equations was treated with second-order upwind difference [40]. The grid near the bottom wall and step was refined to determine the velocity gradient. Scaled residuals for energy and velocity components were set at 10^-6 (0.0001) in Ansys for accurate.

2.3 Boundary Conditions

To analyze the fluid flow and heat transfer performance in the test channel, the following governing equations and boundary conditions are defined, as shown in Eq. (6) - Eq. (17):

The boundary conditions at the inflow section are as follows:

$$u = u_{in}\,, V = 0\,, and\ \theta = 0, T = T_{m_{in}} = 300K \tag{6}$$

$$\text{kin} = \frac{3}{2}(1u_{in})^2, \varepsilon_{in} = c_u \frac{3}{4}\frac{k^{\frac{3}{2}}}{Lt} \tag{7}$$

The fully developed equation presented by Li *et al.,* [43]:

$$\frac{L}{D} = [(0.631)^{1.6} + (0.0442\text{Re})^{1.6}] \tag{8}$$

The conditions at the outlet boundary:

$$\frac{\partial k}{\partial x} = \frac{\partial \varepsilon}{\partial x} = 0\,,\ \frac{\partial T_f}{\partial x} = 0\,,\ \frac{\partial U}{\partial x} = 0, \frac{\partial V}{\partial x} = 0 \tag{9}$$

The wall:

$$u = v = o\,, q = q_{corrugated} \tag{10}$$

For determining the flow and heat transfer characteristics inside the test channel, the following equations are provided. The mean heat transfer coefficient:

$$h = q\,\frac{ln\left(\frac{T\omega - Tm\cdot in}{Tw - Tm_{\ 0\cup T}}\right)}{(Tw - Tm_{in}) - \left(T_\omega\ ^{-\ T}{}_{m_0 u_T}\right)} \tag{11}$$

$$q = \frac{m\ Cp\ (Tw - Tm\,,out\,)}{A} \tag{12}$$

where A represents the corrugated surface area, and Tm;out and Tm;in denote the average inlet and exit temperatures of the working fluid. The velocity at the inlet:

$$u_{in} = \frac{Re\, u}{\rho Dh} \tag{13}$$

The average Nusselt number (*Nu*):

$$Nu = \frac{hD_h}{k} \tag{14}$$

where D_h represents the hydraulic diameter of the channel, determined as follows:

$$D_h = \frac{4A}{P} \tag{15}$$

P denotes the channel's wetted perimeter, whereas A represents the channel's cross-sectional area. The channel's friction factor:

$$f = \frac{2D_h \Delta_P}{L\rho u^2} \tag{16}$$

The Performance Evaluation Criteria (PEC) were utilised to assess the hydraulic and thermal performance of the channel, with the PEC calculated as detailed below:

$$PEC = \frac{(Nu/Nu_0)}{(f/f_\sigma)^{\frac{1}{3}}} \tag{17}$$

In this context, *Nu* signifies the Nusselt number, while *f* indicates the friction factor for the novel channel structure, which consists of a backward-facing step in conjunction with a corrugated wall. Nu^o denotes the Nusselt number, whereas f^0 represents the friction factor for the original channel (backward-facing step) [44].

2.4 Mesh Generation

Mesh Grid independent (228,709)

A network study and code validation were conducted by creating a computational grid using ANSYS V.24 R2. A structural grid, based on a rectangular grid, was chosen for this simulation. To ensure validity and accuracy, various network sizes (25150, 32067, 40603, 61691, 105856, 228709, & 398950) were examined, as shown in Table 1, depicting Reynolds number (*Re*) for pure water with a surface Nusselt number (*Nu*) in seven different networks. The results indicated independence from the number of grid points, and the relative error between the six and seven grids was negligible. Therefore, a grid size of 228709 was utilized, employing a non-uniform grid for computational efficiency. Similar grid independence methods were used by Taib *et al.,* [41] for CFD. The error percentage (e%) was calculated as e%= $\left|\frac{Q-Q_{n-1}}{Q_n-1}\right|$, where Q represents any quantity analyzed. The wall parameter $y^+$was maintained at approximately 1 in all cases, following enhanced wall treatment guidelines. Additional validation was conducted using data from Pehlivan *et al.,* [45] and Elshafei *et al.,* [46], demonstrating the accuracy and reliability of the methodology in predicting heat transfer and flow characteristics in BFS configurations.

Moreover, the code underwent validation through a comparison of its results with experimental data provided by Hilo [47] for fluid flow within a backward-facing step (BFS) channel, encompassing both smooth and corrugated BFS models. The agreement between the CFD numerical results from this study and experiment results of Hilo [47] regarding Nusselt number and pressure drop is notable, as illustrated in Figure 2 (a and b). Additionally, the validation aligns with Asral *et al.,* [48], using benchmark comparisons and error analysis to ensure reliability.

Table 1
Reynolds number (*Re*) for pure water with a surface Nusselt number (*Nu*) in five different networks

Grid No.	Velocity (m/s)	Mesh element size (mm)	Grid nodes	Pressure (pa)	$\boldsymbol{Nu}$	$\boldsymbol{e}$ %
1	0.300901	0.7	25150	58.3398	67.4053	---------
2	0.300901	0.6	32067	58.5378	67.5293	0.1841
3	0.300901	0.5	40603	58.6407	67.6672	0.2042
4	0.300901	0.4	61691	58.6869	67.6940	0.0396
5	0.300901	0.3	105856	59.4497	67.7433	0.0729
6	0.300901	0.2	228709	60.4422	67.7727	0.0433
7	0.300901	0.18	398950	60.6699	67.7741	0.0021

Table 2
Details information of the cases in the code validation studies

Case no.	Author	Channel	Flow	Geometry parameters
1.	Hilo [47]	Backward facing Step Smooth	Turbulent *Re*=5,000 to 20,000	S= 10 mm Upstream=0.2m Downstream=0.3m
2.	Hilo [47]	Backward facing Step trapezoidal	Turbulent *Re*=5,000 to 20,000	S= 10 mm Upstream=0.2m Downstream=0.3m P=20mm, a=4mm

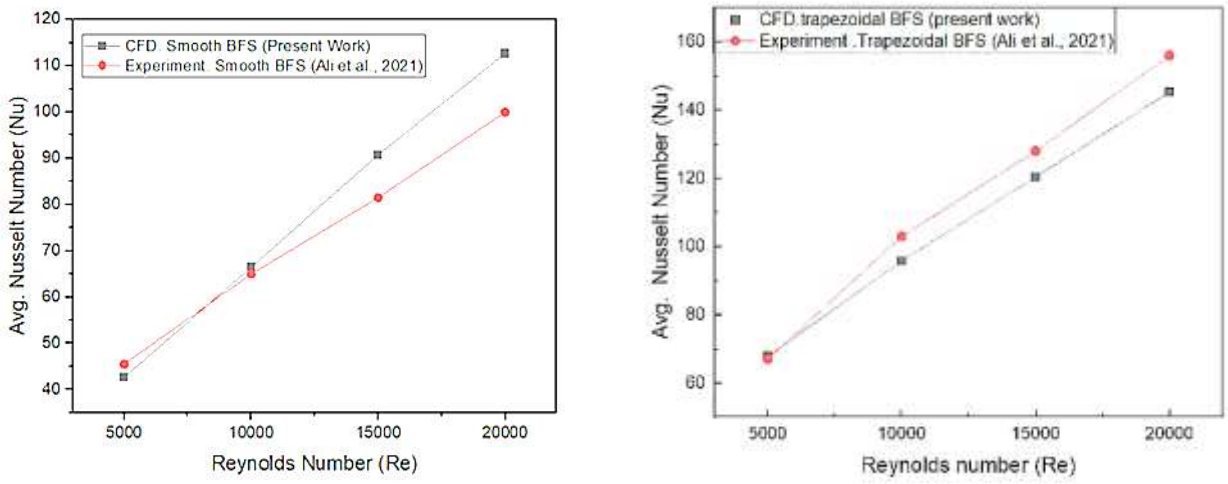

(a) (b)

Fig. 2. Numerical result comparison with previous experiment result (a) average Nusselt number from Hilo [47] (straight channel) (b) average Nusselt number from Hilo [47] (corrugated channel)

3. Results and Discussions

Trapezoidal corrugated walls and various obstacles were observed to affect the thermal and hydraulic performance of a backward facing step (BFS) at constant heat flux across Reynolds numbers

(Re) from 5000 to 20,000. Four models with corrugated walls downstream and obstacles at different locations were studied. The research analysed the effect that different positions of obstacles in the corrugated structures had on heat transfer and fluid flow hydraulic in the channel.

3.1 Effects of Different Obstacle Positions in Corrugated Shapes

The integration of corrugated walls with obstructions in the BFS channel markedly affected fluid dynamics and thermal transfer efficiency. Figures 5(a) and (b) depict the surface Nusselt number (*Nu*) and skin friction coefficient along the corrugated walls and obstacles at a designated Reynolds number (*Re* = 5000), with a pitch diameter of 20 mm and an amplitude height of 4 mm. Notably, the trapezoidal corrugated bottom with obstacles positioned 215 mm from the inlet on the upper wall exhibited the optimum heat transfer and Nusselt number (*Nu*) compared to other geometries with different obstacle positions.

The distribution of skin friction coefficients for corrugated walls with obstacles varied in frequency compared to the corrugated surface with obstacles. The highest and lowest coefficients corresponded to locations with the longest and shortest obstacle lengths and angles relative to the upper wall, indicating diverse flow patterns along the corrugation surface. The presence of obstacles significantly influenced thermal performance and heat transfer by redirecting flow near the wall, promoting mixing of cold and hot flows, and inducing heat gain within vortices. Consequently, the trapezoidal corrugated bottom with obstacles demonstrated superior heat transfer enhancement due to the formation of a larger recirculation region.

Moreover, the trapezoidal shape consistently outperformed other configurations in terms of *Nu* rates, aligning with previous studies. Figure 5(a) depicts higher *Nu* values in the converging sections of each corrugation wave compared to the diverging sections, attributed to elevated velocity gradients and average velocities enhancing heat transfer ratios. *Nu* remained nearly constant after the third corrugation of each channel, signifying fully developed flow conditions.

3.2 Effects of Reynolds Number on Heat Transfer

Figure 6(a) shows the average Nusselt Number (*Nu*) vs Reynolds Number (*Re*) for different obstacle positions in corrugated channels. For all configurations, *Nu* increased with increasing *Re*, indicating higher heat transfer induced by increased turbulence caused by the presence of obstacles in the corrugated walls. In particular, trapezoidal configuration offered better heat transfer compared to other configurations when the obstacle was placed at 215 mm from the inlet. The increase of *Re* enhanced the formation of larger recirculation regions inducing better mixing between hot and cold flows and steepening temperature gradients. As *Re* increased, this turbulence driven recirculation was found to significantly enhance the heat transfer performance, with the trapezoidal configuration being the most effective at maximizing thermal performance [5, 24, 47]. Enhanced thermal mixing, consistent with baffle effects reported by Sadikin *et al.,* [49].

3.3 Effects of Different Obstacle Models on Velocity and Thermal Distribution

Flows through corrugated backward facing step channels at Reynolds number 5000 provide some initial insights of the influence of various obstacle shapes on velocity as well as thermal distribution in these channels. The obstacle configurations greatly affect the velocity distribution as evidenced by the emergence of small recirculation regions near the step corners as in backward facing step channels, as shown in Figure 3. Both the converging and diverging sections of the corrugated walls

and obstacles produce stable secondary vortices for both converging and diverging sections. The most prominent velocity gradient is found behind the backward facing step with trapezoidal corrugated walls for model D, as seen in Figure 3(d).

As depicted in Figure 3(a), model A, the flow separation at the backward facing step is followed by reattachment downstream and results in high velocity zones close to the upper channel wall. This disruption results in thermal boundary layer thinning, and therefore higher Nusselt numbers. With an obstacle in this configuration, the corrugated surface plays an important role in enhancing convective heat transfer. Indeed, sliding velocity gradient in Model B shown in Figure 3(b) is much smoother, with elongated recirculation zone and smoother flow transitions, though heat transfer efficiency is similar to that of Model A.

Although the lower velocity and decreased turbulence leads to lower mixing, circulation is enhanced and stable vortex formation occurs in the extended recirculation zone, producing effective mixing of fluid layers. Such a configuration results in a thinning of the thermal boundary layer along the wall similar to Model A and with the same order of the Nusselt number. As shown in Figure 3(c) model C reduces the velocity gradient even further, leading to a more laminar profile after the step. If the turbulence is reduced, the thickening of the thermal boundary layer reduces heat transfer efficiency. Low velocity in the recirculation region impedes convective heat transfer and further exacerbated the thermal performance of this model.

Finally, model D (Figure 3(d)) exhibits strong flow separation leading to a large recirculation zone and substantial turbulent mixing. This heavily disrupts the boundary layer and produces great enhancement in convective heat transfer as evidenced by a higher Nusselt number. The impact of flow separation and turbulence on pressure drop, as observed by Sadikin *et al.,* [49], aligns with findings in backward-facing step geometries. In applications where heat transfer rates are required to be higher, this model is very suitable.

Yet the velocity distribution near the wall is made richer and the flow mixing in backward facing channels is better in the presence of corrugated walls and obstacles. The effect is more pronounced than in channels with straight steps or corrugations without obstacles. At *Re* 5000, flow dynamics are found to be strongly dependent on obstacle height and corrugation parameters, generating secondary vortices which increase heat transfer.

Models A, B, and D (Figure 3a, 3b, 3d) demonstrate superior thermal performance, while Model C (Figure 3c) shows lower heat transfer due to smoother velocity distribution. These findings emphasize the role of obstacle design in optimizing heat transfer in corrugated channels.

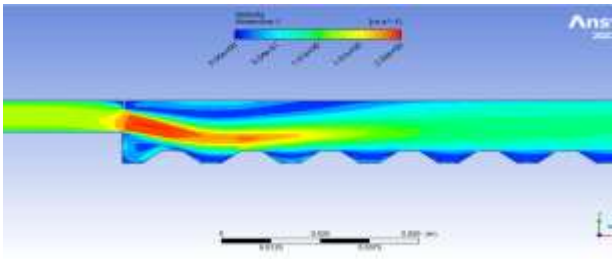

(a)

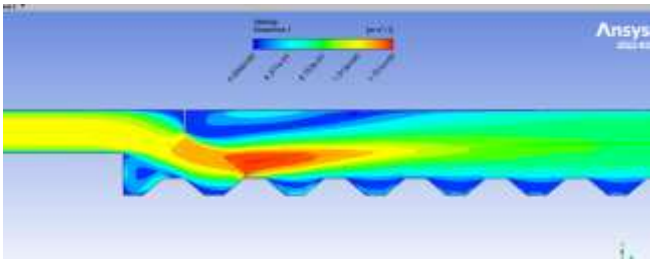

(b)

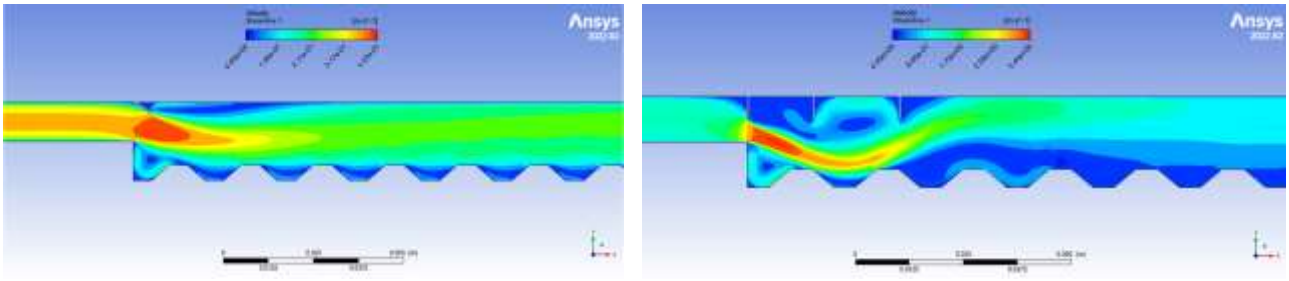

(c) (d)

Fig. 3. displays the velocity streamlines in four backward-facing step trapezoidal corrugated channels: (a) Model A, (b) Model B, (c) Model C, and (d) Model D, at Re = 5000 under 40 kW/m²

The isothermal contours of backward-facing step (BFS) channels with trapezoidal corrugated walls and four obstacle configurations were analyzed at a Reynolds number of 5000 under constant wall heat flux, as shown in Figure 4. Model A (Figure 4(a)), with the obstacle positioned close to the inlet, generates localized recirculation zones near the step corner, enhancing vortex activity and fluid mixing, resulting in moderate heat transfer improvements localized near the inlet. Model B (Figure 4(b)), with the obstacle placed 215 mm from the inlet, demonstrates the most effective fluid mixing, creating an extended recirculation zone that thins the thermal boundary layer at the reattachment point (X ≈ 0.03 m), achieving the highest heat transfer rates among all models.

These findings are consistent with Hilo [47], in that increased secondary vortex strength, increased fluid mixing, and thinning of the thermal boundary layer are effected when amplitude height and wavelength vary. Model B also shows mixing and thermal performance with an extended recirculation zone and optimal placement of the obstacle (X ≈ 0.03m). Contrastingly, Model C (Figure 4(c)), with a 30° angled obstacle, leads to a smoother flow with reduced turbulent nature, a thicker thermal boundary layer, minimal fluid mixing, and hence lowest heat transfer efficiency. Model D (Figure 4(d)), with three obstacles, produces dramatic turbulence and strong secondary vortices, strongly disrupting the thermal boundary layer, producing the highest temperature gradients and greatest heat transfer rates but with higher energy losses. Of the configurations, Model B offered the best compromise of heat transfer performance and energy efficiency.

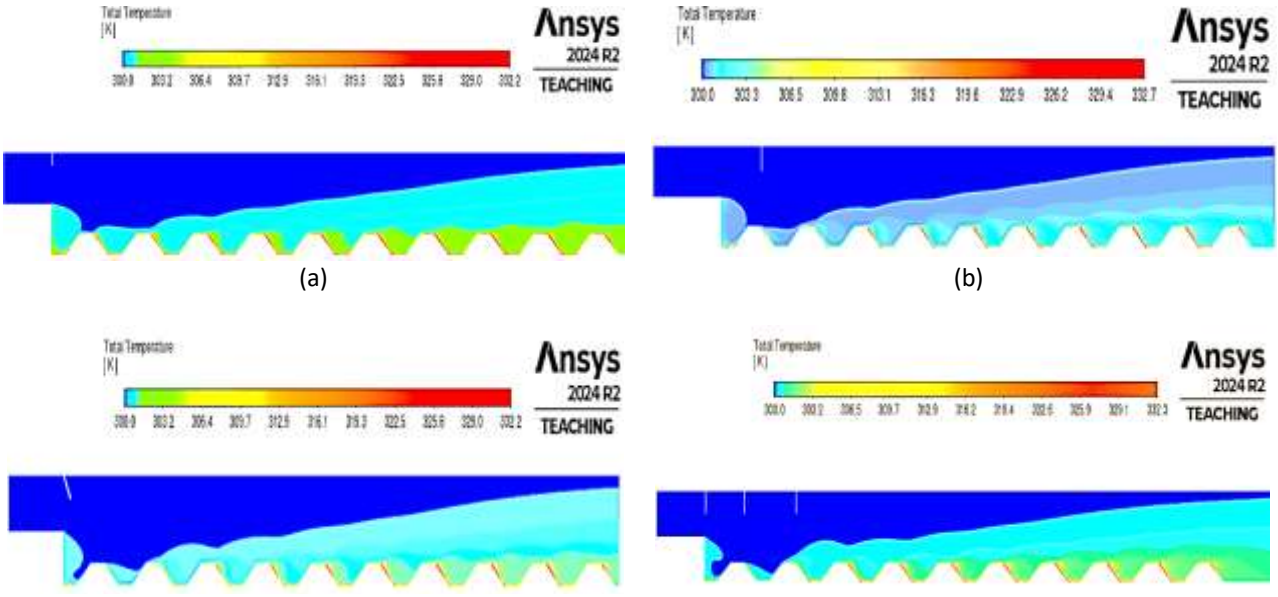

(a) (b)

(c) (d)

Fig. 4. Isothermal contours of four backward-facing step trapezoidal corrugated channels with obstacles: (a) Model A, (b) Model B, (c) Model C, and (d) Model D, at Re = 5,000 and 40 kW/m²

3.4 Effects of Different Obstacle Models on Heat Transfer, Friction Coefficient, and Flow Efficiency

The figures attached display the fluid flow and heat transfer in a system where a corrugated wall combines with obstacles in a backward-facing step, and reveals how the structure affects the flow. The surface Nusselt number (*Nu*) distribution for each model at *Re* = 5000 is shown in Figure 5 (a) and the corresponding skin friction coefficient in Figure 5 (b).

Model D, which has 3 obstacles, achieves the peak *Nu*, up to 292. These increased turbulence and strong recirculation around the obstacles improve fluid mixing and convective heat transfer resulting in this superior heat transfer performance. Model C has the lowest values of *Nu* for 4 models, therefore, smoother flow with less recirculation and less heat transfer efficiency is shown.

The models with obstacles, especially Model D, improve heat transfer significantly relative to the smooth and trapezoidal backward facing step (BFS) configurations. The overall *Nu* for the trapezoidal BFS is moderate but less than for all the obstacle enhanced models; the smooth BFS again exhibits the lowest overall *Nu* due to the absence of flow disturbances.

Figure 6 (b) also shows that Model D has the largest skin friction coefficient of up to 0.0325 in regions characterized by high recirculation and flow separation due to the obstacles. Strong turbulence caused increased friction. On the other hand, Model C possesses lower skin frictions, which suggest smoother flow and hence lower resistance. Skin friction and heat transfer are moderate in both models A and B, yielding an acceptable flow efficiency and thermal performance balance. From a skin friction standpoint the smooth BFS has the lowest skin friction, the trapezoidal BFS slightly exceeds this and is lower than the obstacle enhanced models.

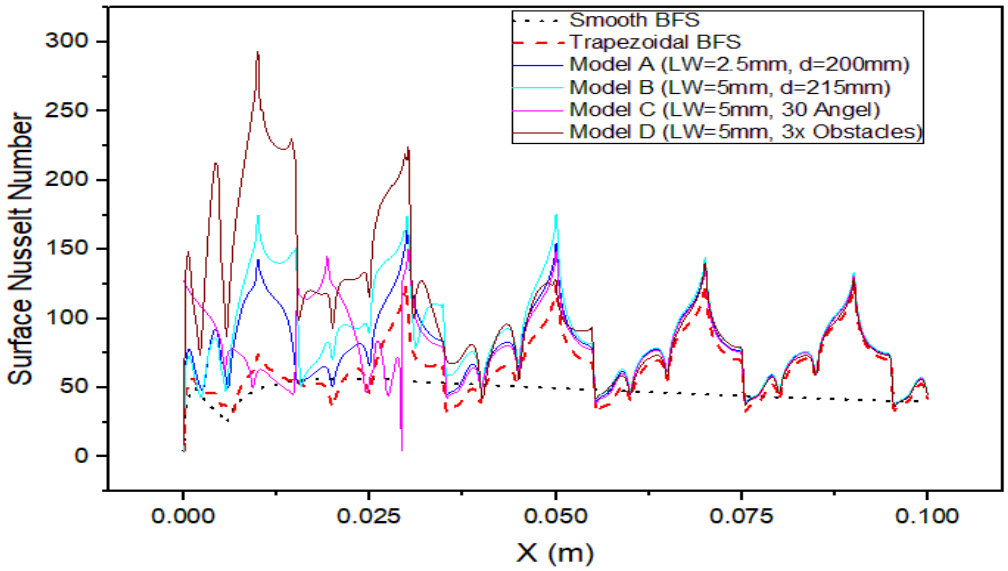

(a)

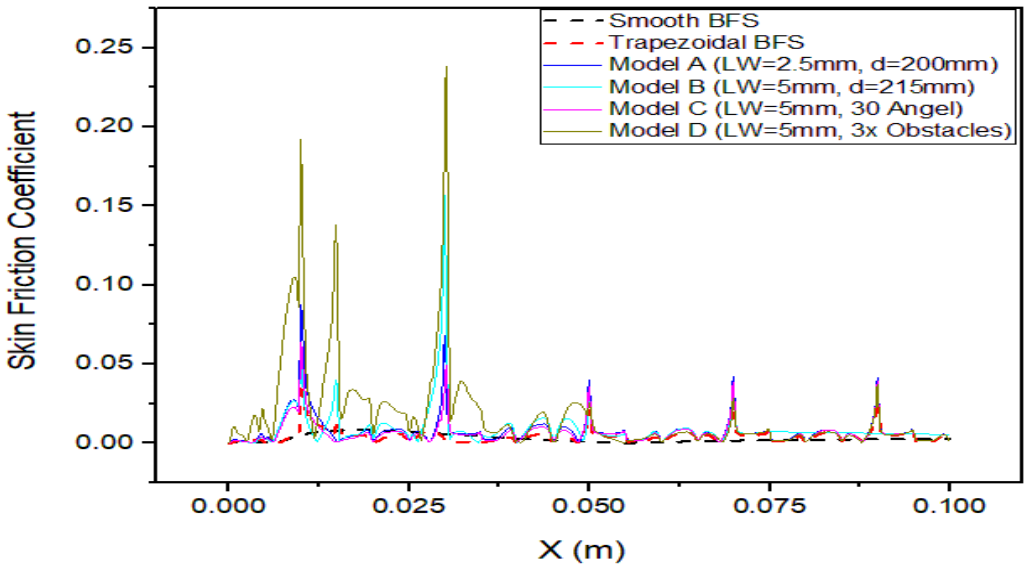

(b)

Fig. 5. The distribution of the surface Nusselt number *Nu* and the skin friction coefficient along the axial direction of the channel at *Re*=5000

At varying Reynolds numbers (5,000 to 20,000), average Nusselt number, skin friction coefficient, pressure, and performance evaluation criterion (PEC) are analyzed for four BFS corrugated channels with four different obstacle configurations in Figure 6. The testing was done at constant wall heat flux (40 kW/m²) with water as the working fluid.

However, model D, which includes three obstacles, has the highest average Nusselt number for all Reynolds numbers, starting with 88.6 (*Re* 5000), and increasing up to 211.1 (*Re* 20000), as shown in Figure 6(a). This high value demonstrates excellent heat transfer as a result of increased turbulence and recirculation resulting from the obstacles. The obstacles that cause turbulence and increase recirculation resulted in the thermal boundary layer to be disrupted leading to a large increase in Nusselt number with increasing Reynolds numbers. On the other hand, Model C (Figure 6(a) with the 30° angle obstacle) has the poorest heat transfer performance with Nusselt numbers of 75.7 (*Re* 5000) and 170.2 (*Re* 20000). Figure 6(a) shows that Model B has moderate heat transfer of 80.7 (Re 5000), and 181.9 (*Re* 20000); and Model A has similar value of 78.4 (*Re* 5000), and 186.8 (*Re* 20000).

According to the second Figure 5(b), Model D has the highest skin friction, shown in Figure 6(b), starting at 0.01125 (*Re* 5000) and ending at 0.00591 (*Re* 20000). In the case of the three-obstacle configuration there are more flow disturbances, as well as interaction with the wall, which results in an increase in the friction. At higher Reynolds numbers, the flow makes a transition to a more turbulent regime, reducing frictional resistance versus flow momentum and hence skin friction is reduced with increasing Reynolds numbers. In another front Model C has the lowest skin friction starting with 0.00582 (*Re* 5000) and decreasing to 0.00271 (*Re* 20000) corresponding to its smoother flow and lower heat transfer rates.

The highest pressure, that is, peaking at 3500 Pa (*Re* = 20000), is achieved in model D, Figure 6 (d), due to high turbulence created by 3x obstacles. The less aggressive obstacle configurations of models C and B are associated with easier flow and therefore with lower pressures (around 1032 Pa & 1121 Pa).

Interestingly, despite Model D's superior Nusselt number and high friction, Model B achieves, as shown in Figure 6(c), the highest PEC (1.67 at *Re* 5000), followed closely by Model C (1.61). This implies that although Model D with 3x obstacles has the best heat transfer, its higher friction reduces

its overall efficiency. However, Model B (Lw=5mm, d=215mm) is more efficient while achieving a better balance between heat transfer and friction.

BFS corrugated channel obstacle design is emphasized to optimize heat transfer and flow efficiency in these results.

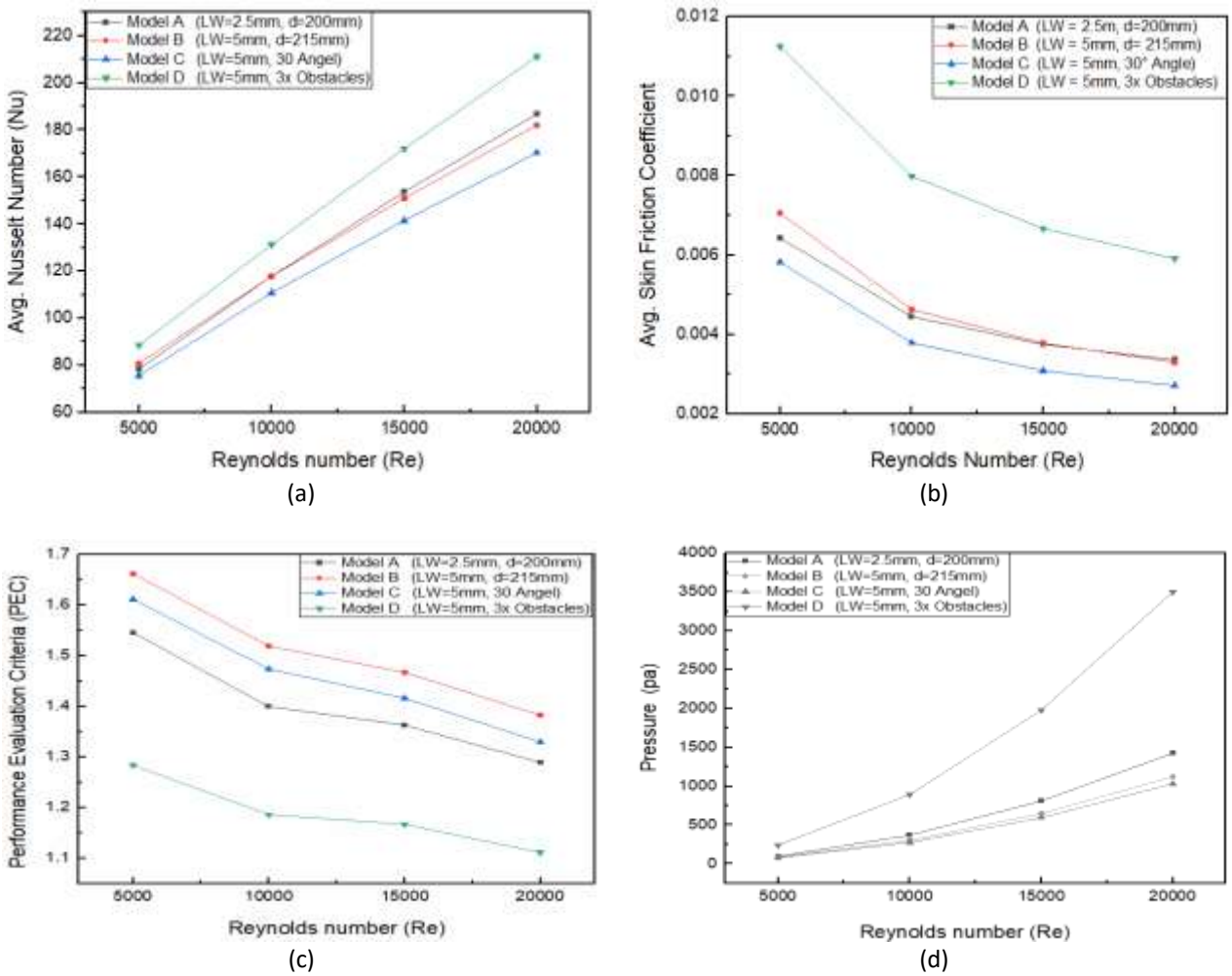

Fig. 6. Variation of (a) average Nusselt number, (b) skin friction factor, (c) performance evaluation criteria, and (d) pressure with increasing Reynolds number from 5,000 to 20,000 for four BFS corrugated channels integrated with obstacles, including d=200mm, d=215mm, 30^{o} angle, and three obstacles, using water as the fluid, at constant wall heat flux = 40k W/m2

3.5 Performance Evaluation Criteria

Selection of high-performance evaluation criteria allows for much more efficient, cost effective and sustainable operation of heat transfer systems by striking a dynamic balance of heat transfer enhancement and frictional losses. BFS Model B (Lw=5mm, d=215mm) or BFS Model C (Lw=5mm, 30° angle) may be more attractive for superior overall performance because their relatively higher evaluated performance criteria include consideration of both heat transfer and frictional loss. So, we select Model B having 5mm Lw and 215mm d from the above comparison because, although the pressure drop is more, Model B has high Nusselt number compared to Model C.

3.6 Alignment of BFS Modifications with Present Findings

The Table 3 below demonstrates that geometric modifications and flow-interrupting elements consistently enhance heat transfer, aligning closely with the findings of the present study.

Table 3
Comparative Analysis of Heat Transfer Enhancements in Backward-Facing Step (BFS) Geometries with Modifications

	Authors	Geometry / Modifications	Findings
1	Abdollahpour *et al.,* [50]	BWFS with and without a rigid cylinder downstream of the step	-BWFS With Cylinder showed increased maximum velocity values compared to BWFS Without Cylinder.
2	Alkumait *et al.,* [51]	Backward-facing step channel with a baffle installed on the upper wall. The baffle's position is varied at three distances downstream from the step: d1=40 mmd, d2=70 mm, and d3=100 mm	-The addition of a baffle significantly improves heat transfer, with a maximum enhancement of 213% for d1=40 mmd
3	Azeez *et al.,* [20]	Flat, backward-facing step, triangular, and trapezoidal channels with corrugated walls	- Trapezoidal channels achieved a 30% heat transfer enhancement with 4% nanofluid compared to pure water
4	Bouazizi *et al.,* [52]	A 2D backward-facing step (BFS) channel with an adiabatic square cylinder placed in the primary recirculation zone, sized at 1/4 of the channel width	-At φ=0.04, Nu increases by 4.91% (CuO), 4.48% (Al_2O_3), and 3.76% (ZnO) without a square cylinder, rising to 17.14%, 16.69%, and 15.84% with a square cylinder.
5	Eleiwi *et al.,* [3]	Backward facing step with three adiabatic non-rotating circular cylinders	-Heat transfer improves by 6% at *Re*=50 and by 13% at *Re*=250. -The Nusselt number exhibits a notable increase with rising Reynolds number and heat flux, with the maximum Nusselt number observed downstream of the second cylinder.
6	Fathinia *et al.,* [10]	Backward-facing step channel with four blockage shapes: circular, back-facing triangular, front-facing triangular, and trapezoidal	- Blockage shapes significantly influence thermal and fluid flow characteristics over backward-facing steps. -Front-facing triangular blockage had the highest Nusselt number (~12% higher than circular blockage at *Re* = 200).
7	Hilo [47]	A trapezoidal corrugated wall in conjunction with a backward-facing step (BFS) channel. Amplitude heights (1–5 mm) and wavelengths (10–60 mm) are among the parameters that have been examined.	-Corrugated walls increased the average Nusselt number (Nu) by up to 40.7% compared to smooth BFS. -Highest heat transfer observed at amplitude height a=4 and wavelength λ=20 mm.
8	Ma *et al.,* [24]	Forward- and backward-facing steps channel with a baffle installed on the top wall. Various baffle lengths ($0 \le h \le 1.5$) and positions ($3 \le X_2 \le 7$) were analyzed.	-Incorporating baffles in forward- and backward-facing step channels significantly enhances heat transfer, especially with hybrid nanofluids. -Maximum average Nusselt number achieved with baffle length h=1.5h = 1.5h=1.5 and position X2=3X_2 = 3X2=3.

4. Conclusion

In this study, the effect of trapezoidal corrugated walls and different arrangements of the obstacles to the thermal and hydraulic performance of a backward-facing step (BFS) channel under constant wall heat flux was investigated for a wide range of Reynolds number from 5000 to 20,000. Four different obstacle positions were studied as models of the corrugated wall with different obstacle positions. The results showed how obstacle positions affect heat transfer and fluid flow dynamics, giving advice on the design of BFS channels for thermal improvements.

Analysis showed that the best overall heat transfer performance was for the BFS Model B in which the obstruction was located 215 mm from the inlet and wall length was 5 mm. With this configuration the second higher average Nusselt number (Nu) over the Reynolds number range was observed which implies higher heat transfer rates.

Forced by the strategic location of the obstacle, the obstacle induced a recirculation region which enhances the mixing between hot and cold flow layers, and thus improving the thermal efficiency. Furthermore, velocity streamlines of Model B depicted less count of thermal boundary layer thickness reduction which in turn results in better heat transfer.

While BFS Model D (three obstacles) gave the highest Nusselt number in a few cases, it caused the highest skin friction coefficient thereby generating largest frictional losses. Model B has the best performance evaluation criteria (which is a balance between frictional losses and heat transfer enhancements) and the best overall heat transfer performance while Model C (30° angle obstacle) has the lowest skin friction factor, not necessarily the lowest for the most part.

Through performance evaluation, BFS Model B (Lw = 5 mm, d = 215 mm) emerged as optimal for enhancing heat transfer in BFS channels. Model B achieves high thermal performance with low friction losses, making it suitable for applications requiring efficient heat transfer and compensatory thermal performance in optimized configurations.

Variations in obstacle shapes and configurations could be taken up for further studies to better refine heat transfer performance. Moreover, the application of the models in laminar flow conditions or with other working fluids could shed light on potential broader applications of the results.

5. Limitations and Future Study

This study illustrates dramatic heat transfer enhancement using trapezoidal corrugated walls and obstacles at a location 215 mm from the inlet, for one fluid (water) and Reynolds numbers of 5000–20,000, but the results are specific to particular configurations. The situation may vary depending on the fluid properties, obstacle geometries and conditions. Future research should also be investigated through focusing on alternative fluids, larger Reynolds number ranges, and a wider variety of obstacle designs. Better capturing complex flow patterns and thermal gradients from more realistic mechanical aspect would take us to 3D simulations instead. Further, investigations are needed to characterize the flow field, pressure drop, drag and system efficiency for a more effective engineering evaluation for potential industrial purposes.

Acknowledgement
This research was not funded by any grant.

References

[1] Jiménez, Araceli Sánchez, Raquel Puelles, Marta Perez-Fernandez, Leire Barruetabeña, Nicklas Raun Jacobsen, Blanca Suarez-Merino, Christian Micheletti et al. "Safe (r) by design guidelines for the nanotechnology industry." *NanoImpact* 25 (2022): 100385. https://doi.org/10.1016/j.impact.2022.100385

[2] Mohammad Jokari, Reza Bahoosh Kazerooni, Reza Khalili, and Ebrahim Tavousi. "Simulating flows in backward-facing step for various expansion ratios by finite element-lattice Boltzmann." *Physics of Fluids* 36, no. 7 (2024): https://doi.org/10.1063/5.0212599

[3] Muhammad Asmail Eleiwi, Tahseen Ahmad Tahseen, and Ayad Fouad Hameed. "Numerical study of fluid flow and heat transfer in a backward facing step with three adiabatic circular cylinder." *Journal of Advanced Research in Fluid Mechanics and Thermal Sciences* 72, no. 1 (2020): 80-93. https://doi.org/10.37934/arfmts.72.1.8093

[4] Recep Ekiciler, Emre Aydeniz, and And Kamil Arslan. "The effect of volume fraction of Sio2 nanoparticle on flow and heat transfer characteristics in a duct with corrugated backward-facing step." *Thermal Science* 22 (2018): S1435-S1447. https://doi.org/10.2298/TSCI18S5435E

[5] Hussein A. Mohammed, F. Fathinia, Hari B. Vuthaluru, and Shaomin Liu. "CFD based investigations on the effects of blockage shapes on transient mixed convective nanofluid flow over a backward facing step." *Powder Technology* 346 (2019): 441-451. https://doi.org/10.1016/j.powtec.2019.02.002

[6] Nie, J. H., and Bassem F. Armaly. "Three-dimensional convective flow adjacent to backward-facing step-effects of step height." *International journal of heat and mass transfer* 45, no. 12 (2002): 2431-2438. https://doi.org/10.1016/S0017-9310(01)00345-3

[7] Jehad, D. G., G. A. Hashim, A. Kadhim Zarzoor, and CS Nor Azwadi. "Numerical study of turbulent flow over backward-facing step with different turbulence models." *Journal of Advanced Research Design* 4, no. 1 (2015): 20-27.

[8] Sadeq Salman, Abd Rahim, Abu Talib, Ali Hilo, Sadeq Rashid Nfawa, Mohamed Thariq, Hameed Sultan, and Syamimi Saadon. "Numerical Study on the Turbulent Mixed Convective Heat Transfer over 2D Microscale Backward-Facing Step." *CFD Letters* 10 (2019): 31-45.

[9] Boudiaf, Ahlem, Fetta Danane, Youb Khaled Benkahla, W. Berabou, M. Benzema, N. Labsi, and S-E. Ouyahia. "Numerical study of viscous dissipation and non-Boussinesq model effects on CMC–TiO 2 fluid flow over backward facing step with baffle." *Journal of Thermal Analysis and Calorimetry* 135 (2019): 787-799. https://doi.org/10.1007/s10973-018-7479-1

[10] Fathinia, F., and Ahmed Kadhim Hussein. "Effect of blockage shape on unsteady mixed convective nanofluid flow over backward facing step." *CFD Letters* 10, no. 1 (2018): 1-18.

[11] Afrah Turki Awad, Abdulelah Hameed Yaseen, and Adnan M Hussein. "Evaluation of Heat Transfer and Fluid Dynamics across a Backward Facing Step for Mobile Cooling Applications Utilizing CNT Nanofluid in Laminar Conditions." *CFD Letters* 16, no. 10 (2024): 140-153. https://doi.org/10.37934/cfdl.16.10.140153

[12] Jincheng Zhang, Zhenguo Wang, Mingbo Sun, Hongbo Wang, Chaoyang Liu, and Jiangfei Yu. "Effect of the backward facing step on a transverse jet in supersonic crossflow." *Energies* 13, no. 6 (2020): https://doi.org/10.3390/en13164170

[13] Ashwin Sivan, D. Saravanan, and Y. S. Rammohan. "A numerical study to reduce the drag effects in hypersonic flow over the backward facing step." *Materials Today: Proceedings* 52 (2022): 963-970. https://doi.org/10.1016/j.matpr.2021.10.429

[14] Xie, W. A., and G. N. Xi. "Flow instability and heat transfer enhancement of unsteady convection in a step channel." *Alexandria Engineering Journal* 61, no. 9 (2022): 7377-7391. https://doi.org/10.1016/j.aej.2022.01.007

[15] Alawi, O. A., NA Che Sidik, S. N. Kazi, and M. Kh Abdolbaqi. "Comparative study on heat transfer enhancement and nanofluids flow over backward and forward facing steps." *Journal of Advanced Research in Fluid Mechanics and Thermal Sciences* 23, no. 1 (2016): 25-49.

[16] Lachlan J. JardineRobert J. Miller. "The Effect of Heat Transfer on Turbine Performance." *Mechanical Engineering* 142, no. 9 (2020): 56-57. https://doi.org/10.1115/1.2020-SEP5

[17] Reddy, D. Siva Krishna, Pankaj Kumar, Jai Makhija, Amjad Ali Pasha, and Abdul Zubar Hameed. "CFD of flow dynamic and heat transfer characteristics of dual step cylinders at Re= 2100." *Arabian Journal for Science and Engineering* 46, no. 12 (2021): 12667-12683. https://doi.org/10.1007/s13369-021-06029-0

[18] Kevin Ignatowicz, Elie Solaï, François Morency, and Héloïse Beaugendre. "Data-Driven Calibration of Rough Heat Transfer Prediction Using Bayesian Inversion and Genetic Algorithm." *Energies* 15, no. 10 (2022): https://doi.org/10.3390/en15103793

[19] Alberto F. Rius-VidalesM. Kotsonis. "Impact of a forward-facing step on the development of crossflow instability." *Journal of Fluid Mechanics* 924 (2021): https://doi.org/10.1017/jfm.2021.497

[20] Kafel Azeez, Abd Rahim Abu Talib, and Riyadh Ibraheem Ahmed. "Heat transfer enhancement for corrugated facing step channels using aluminium nitride nanofluid - numerical investigation." *Journal of Thermal Engineering* 8 (2022): 734-747. https://doi.org/10.18186/thermal.1197106

[21] Koca, Ferhat. "Numerical investigation of corrugated channel with backward-facing step in terms of fluid flow and heat transfer." *Journal of Engineering Thermophysics* 31, no. 1 (2022): 187-199.https://doi.org/10.1134/S1810232822010143

[22] Fatih SelimefendigilHakan F. Öztop. "Forced convection and thermal predictions of pulsating nanofluid flow over a backward facing step with a corrugated bottom wall." *International Journal of Heat and Mass Transfer* 110 (2017): 231-247. https://doi.org/10.1016/j.ijheatmasstransfer.2017.03.010
[23] Ayad S. Abedalh, Zaid A. Shaalan, and Husam Naufal Saleh Yassien. "Mixed convective of hybrid nanofluids flow in a backward-facing step." *Case Studies in Thermal Engineering* 25 (2021): https://doi.org/10.1016/j.csite.2021.100868
[24] Yuan Ma, Rasul Mohebbi, Mohammad Mehdi Rashidi, Zhigang Yang, and Yuhao Fang. "Baffle and geometry effects on nanofluid forced convection over forward- and backward-facing steps channel by means of lattice Boltzmann method." *Physica A: Statistical Mechanics and its Applications* 554 (2020): https://doi.org/10.1016/j.physa.2020.124696
[25] Bala Kawa M. Saleem, Andam Mustafa, Dalshad Ahmed Kareem, Mehmet Ishak Yuce, Michał Szydłowski, and Nadhir Al-Ansari. "Numerical Analysis of Turbulent Flow over a Backward-facing Step in an Open Channel." *Archives of Hydroengineering and Environmental Mechanics* 70 (2023): 49-69. https://doi.org/10.2478/heem-2023-0004
[26] Fatih SelimefendigilHakan F. Öztop. "Numerical study of forced convection of nanofluid flow over a backward facing step with a corrugated bottom wall in the presence of different shaped obstacles." *Heat Transfer Engineering* 37 (2016): 1280-1292. https://doi.org/10.1080/01457632.2015.1119617
[27] Masuji Sakaya, Tsuneaki Motai, Masataka Mochizuki, and Kouichi Mashiko, *Corrugated heat pipe*. 1990.
[28] Hamed Sadighi DizajiSamad Jafarmadar. "Experiments on New Arrangements of Convex and Concave Corrugated Tubes through a Double-pipe Heat Exchanger." *Experimental Heat Transfer* 29, no. 5 (2016): 577-592. https://doi.org/10.1080/08916152.2015.1046015
[29] Yan Cao, Phong Thanh Nguyen, Kittisak Jermsittiparsert, Hafedh Belmabrouk, Sayer O. Alharbi, and Mir Saleh Khorasani. "Thermal characteristics of air-water two-phase flow in a vertical annularly corrugated tube." *Journal of Energy Storage* 31 (2020): https://doi.org/10.1016/j.est.2020.101605
[30] Saša Kenjereš. "Heat transfer enhancement induced by wall inclination in turbulent thermal convection." *Physical Review E - Statistical, Nonlinear, and Soft Matter Physics* 92, no. 5 (2015): https://doi.org/10.1103/PhysRevE.92.053006
[31] Sang Wook Han, Young Yun Woo, Taekyung Lee, Jeong Kim, Ji Hwan Jeong, and Young Hoon Moon. "Manufacturing of a corrugated double-layered tube for the high-performance compact heat exchanger." *International Journal of Advanced Manufacturing Technology* 112, no. 7-8 (2021): 2065-2080. https://doi.org/10.1007/s00170-020-06419-y
[32] Nesreen GhaddarAhmad El-Hajj. "Numerical study of heat transfer augmentation of viscous flow in corrugated channels." *Heat Transfer Engineering* 21, no. 5 (2000): 35-46. https://doi.org/10.1080/01457630050127937
[33] Pooja Dutta, Partha Pratim Dutta, and Paragmoni Kalita. "Thermohydraulic investigation of different channel height on a corrugated heat exchanger." *AIP Conference Proceedings* 2091 (2019): https://doi.org/10.1063/1.5096502
[34] Shaofei Zheng, Tingwu Ji, Gongnan Xie, and Bengt Sundén. "On the improvement of the poor heat transfer lee-side regions of square cross-section ribbed channels." *Numerical Heat Transfer; Part A: Applications* 66 (2014): 963-989. https://doi.org/10.1080/10407782.2014.894396
[35] Khudheyer S. Mushatet. "Simulation Of turbulent flow and heat transfer over a backward-facing step with ribs turbulators." *Thermal Science* 15 (2011): 245-255. https://doi.org/10.2298/TSCI090926044M
[36] Hui Xiao, Zhichun Liu, and Wei Liu. "Turbulent heat transfer enhancement in the mini-channel by enhancing the original flow pattern with v-ribs." *International Journal of Heat and Mass Transfer* 163 (2020): https://doi.org/10.1016/j.ijheatmasstransfer.2020.120378
[37] Hamdi Selçuk ÇelikL. Berrin Erbay. "Heat transfer enhancement using different types of turbulators on the heat exchangers." *Journal of Thermal Engineering* 7 (2021): 1654-1670. https://doi.org/10.18186/thermal.1025921
[38] Karrar A. Hammoodi, Hadeel Ali Hasan, Muntadher H. Abed, Ali Basem, and Ammar M. Al-Tajer. "Control of heat transfer in circular channels using oblique triangular ribs." *Results in Engineering* 15 (2022): https://doi.org/10.1016/j.rineng.2022.100471
[39] Younes Menni, Ahmed Azzi, Ali J. Chamkha, and Souad Harmand. "Effect of wall-mounted V-baffle position in a turbulent flow through a channel: Analysis of best configuration for optimal heat transfer." *International Journal of Numerical Methods for Heat and Fluid Flow* 29 (2019): 3908-3937. https://doi.org/10.1108/HFF-06-2018-0270
[40] Ali Kareem Hilo, Abd Rahim Abu Talib, Antonio Acosta Iborra, Mohammed Thariq Hameed Sultan, and Mohd Faisal Abdul Hamid. "Effect of corrugated wall combined with backward-facing step channel on fluid flow and heat transfer." *Energy* 190 (2020): https://doi.org/10.1016/j.energy.2019.116294
[41] Ishkrizat Taib, Nurnabila Syuhada Azian, Norhasikin Ismail, Chuan Huat Ng, and Ridwan Abdurrahman. "Heat Transfer in The Energy Storage during Solidification." *Journal of Advanced Research in Numerical Heat Transfer* 26, no. 1 (2024): 114-127. https://doi.org/10.37934/arnht.26.1.114127

[42] Asral Asral, Nur Maizatul Hanisha Khairi Azhar, Amin Faiq Ahmad Daud, Ishkrizat Taib, Mohamad Saiful Nazri, Hishamuddin Rashid, and Norhasikin Ismail. "Enhanced Thermal Performance of Solar Heating Systems using Phase Change Materials in Stratified Water Storage Tanks." *Advances in Fluid, Heat and Materials Engineering* 1, no. 1 (2024): 1-9.

[43] Zhuo Li, Ya Ling He, Gui Hua Tang, and Wen Quan Tao. "Experimental and numerical studies of liquid flow and heat transfer in microtubes." *International Journal of Heat and Mass Transfer* 50, no. 17-18 (2007): 3447-3460. https://doi.org/10.1016/j.ijheatmasstransfer.2007.01.016

[44] Mahmoud JourabianMehrdad Raeesi. "Turbulent forced convection flow of water-based nanofluids with temperature-dependent properties over backward-facing step channel with upwardly deflected downstream wall." *Numerical Heat Transfer; Part A: Applications* (2023): https://doi.org/10.1080/10407782.2023.2287541

[45] Pehlivan, H., I. Taymaz, and Y. Islamoğlu. "Experimental study of forced convective heat transfer in a different arranged corrugated channel." *International Communications in Heat and Mass Transfer* 46 (2013): 106-111. https://doi.org/10.1016/j.icheatmasstransfer.2013.05.016

[46] Elshafei, E. A. M., M. M. Awad, E. El-Negiry, and A. G. Ali. "Heat transfer and pressure drop in corrugated channels." *Energy* 35, no. 1 (2010): 101-110. https://doi.org/10.1016/j.energy.2009.08.031

[47] Ali Kareem Hilo. "Fluid flow and heat transfer over corrugated backward facing step channel." *Case Studies in Thermal Engineering* 24 (2021): 100862.

[48] Muhammad Asral, Nurnabila Syuhada Azian, Ishkrizat Taib, Shunfann Wu, Wee Hang Yap, Swee Hong Yeap, Feblil Huda, and Awaludin Martin. "CFD Analysis on Double Leaks of Subsea Pipeline Leakage." *Advances in Fluid, Heat and Materials Engineering* 1, no. 1 (2024): 10-26.

[49] Sadikin, A., N. Y. Khian, Y. P. Hwey, H. Y. Al-Mahdi, I. Taib, A. N. Sadikin, S. Md Salleh, and S. S. Ayop. "Effect of number of baffles on flow and pressure drop in a shell side of a shell and tube heat exchangers." *Journal of Advanced Research in Fluid Mechanics and Thermal Sciences* 48, no. 2 (2018): 156-164.

[50] Milad Abdollahpour, PAOLA Gualtieri, and CARLO Gualtieri. Influence of a Rigid Cylinder on Flow Structure over a Backward-Facing Step. in Proceedings of the 39th IAHR World Congress. 2022.

[51] Aadel Abdul Razzaq Alkumait, Maki Haj Zaidan, and Thamir Khalil Ibrahim. "Numerical investigation of forced convection flow over backward facing step affected by a baffle position." *Journal of Advanced Research in Fluid Mechanics and Thermal Sciences* 52, no. 1 (2018): 33-45.

[52] Bouazizi, L., and S. Turki. "Effect of Brownian motion on flow and heat transfer of nanofluids over a backward-facing step with and without adiabatic square cylinder." *Thermophysics and Aeromechanics* 25 (2018): 445-460. https://doi.org/10.1134/S0869864318030113